INTERNATIONAL JOURNAL OF INTEGRATED ENGINEERING
ISSN: 2229-838X e-ISSN: 2600-7916

IJIE

Vol. 16 No. 1 (2024) 26-34
https://publisher.uthm.edu.my/ojs/index.php/ijie

Briquette Shape Roles in Carbothermal Reduction Process of Limonitic Laterite Nickel

Fakhreza Abdul[1], Afif Maulana Yusuf Ridarto[1], Vuri Ayu Setyowati[2], Yuli Setiyorini[1], Sungging Pintowantoro[1]*

[1] *Department of Materials and Metallurgical Engineering,*
Faculty of Industrial Technology and System Engineering,
Institut Teknologi Sepuluh Nopember, Arief Rahman Hakim Street, Surabaya, 60111, INDONESIA
[2] *Department of Mechanical Engineering,*
Institut Teknologi Adhi Tama Surabaya, Surabaya, 60117, INDONESIA

*Corresponding Author: sungging@mat-eng.its.ac.id
DOI: https://doi.org/10.30880/ijie.2024.16.01.003

Article Info

Received: 25 November 2023
Accepted: 11 January 2024
Available online: 25 April 2024

Keywords

Carbothermic reduction, shape of briquette, sustainable process, alternative nickel sources, laterite

Abstract

Lateritic ore carbothermal reduction is currently the focus of many researchers. This process uses a relatively lower temperature of operation than the smelting. Therefore, the carbothermal reduction process has a relatively lower primary energy demand and CO_2 gas emissions. This research examines the appropriate briquette form to obtain the optimum recovery, concentration of nickel, and selective reduction of nickel, as well as analyzes the compounds/phases formed. The briquette in this study was formed into three different geometries, i.e., the pillow, spherical, and cylindrical forms. First, this research was carried out by mixing the raw materials and forming it into specified briquette forms. Second, the formed briquettes were put into a crucible. Third, the coal-limestone bed mixture was used to cover the briquettes. Then, the carbothermic reduction process was started by heating to 700 ^oC for 2 hours and continued to 1400 ^oC for 6 hours. Finally, the magnetic separation process was performed to separate the reduced briquettes. As a result, the cylindrical shape briquette obtained better results at 6.74% Ni, with a nickel recovery of 96.20% and a selectivity factor value of 10.39. The compounds formed after carbothermic reduction process products include FeNi, Fe_3Si, and SiO_2. In a spherical-shaped briquette, Fe_3O_4 and Mg_2SiO_4 were found in the reduced product, indicating impurities in the reduced briquettes.

1. Introduction

The increasing demand for Electric Vehicles (EVs) has led to increasing demand for nickel-based batteries [1]. In its application for EVs, in recent times, nickel-based batteries are still a priority option for EV manufacturing, especially for hybrid-type EVs [2]. As a result, nickel demand is predicted to experience an increasing trend shortly [3]. Laterite nickel is a primary nickel source that is currently the concern of many researchers. It is because of its greater availability in nature compared to sulfide nickel ores [4]. In order to process laterite nickel ores, several options can be used, including proven technologies that run on a commercial scale. Examples of these technologies are Rotary Kiln-Electric Furnace (RK-EF) technology [5], blast furnace [6], or High-Pressure Acid Leaching (HPAL) [7] depending on whether the nickel ore is saprolite or limonite.

Although existing technologies have proven for decades to be effective and economical in processing lateritic nickel ores, researchers are now studying the carbothermic reduction of lateritic nickel ores with lower operating temperatures than RK-EF or Blast Furnace smelting processes. The process is a combination of a direct reduction process followed by a physical separation process through magnetic separation, such as studies from following researchers [8-11]. A direct reduction technology like these studies has existed for a long time in Japan, namely at the Oheyama works [12]. However, along with the global policy to reduce energy and CO_2 gas emissions in the industrial sector, research on the nickel ore direct reduction has become increasingly attractive in recent years. The carbothermic reduction process uses relatively lower temperatures than the smelting process. Therefore, from an environmental point of view, this process has a relatively lower primary energy demand and CO_2 gas emissions than the smelting process. In addition, the products from the carbothermal reduction process can be used for further processing, such as for stainless steel through the pyrometallurgical process or for nickel and cobalt sulfate powder production through the hydrometallurgical process.

Research on carbothermic reduction of lateritic nickel ores followed by magnetic separation has mostly focused on the effectiveness of using additives to improve nickel reduction selectivity combined with the use of optimal reduction temperatures and times [13] and briquetting pressure [14]. Additives that can be used for the process include Na_2SO_4, Na_2CO_3, and NaCl [15], $CaSO_4$ [16], $CaCl_2$ [17], $Na_2S_2O_3$ and sulfur [18], gypsum [19], and others. However, the shape or geometry of laterite nickel ore briquettes is rarely studied. The shape of the briquette is essential for designing operations when this direct reduction technology will be scaled up in pilot plants or commercial-scale research. In addition, the shape of the briquette will affect the reductant gas flow and heat transfer that occurs during the carbothermal reduction process [20, 21]. This research studies the effect of briquette shape of lateritic ore in the carbothermal reduction process. In order to study this, several things will be observed, including nickel content after the reduction process, compounds formed, nickel recovery after the reduction process, and nickel selectivity factors.

2. Materials and Method

2.1 Raw Materials and Chemical Additives

Coal as a reductant and laterite ore as a source of nickel are obtained from areas in Indonesia, namely from Sulawesi and Kalimantan. Meanwhile, limestone was purchased from East Java, Indonesia. An elemental composition characterization and X-Ray examination were accomplished to get the elemental composition and constituent compound mineral of laterite nickel, as presented in Fig. 1 and Table 1. The coal, employed as the reductant and carbon source, was firstly passing anlysis of proximate, as tabulated in Table 2. Furthermore, Table 3 provides the elemental content of limestone. Calcite compounds are the main compounds that make up the limestone. Calcite will then be decomposed when heating which produces CO_2 gas. Then this CO_2 gas will react with C (inside coal) to produce reductant gas (CO). Sodium sulfate (Na_2SO_4) and tapioca were used as chemical additives organic binders, respectively.

Table 1 *Elemental matter of limonitic laterites nickel*

Element	Fe	O	Si	Mg	Al	Ca	Ni	Cr
Wt%	42.01	25.89	17.78	5.91	2.50	2.36	1.59	1.29

Table 2 *Analysis of proximate result of coal reductant*

Parameter	Result	Unit	Standards
Ash Content	1.7	% ar	ASTM D3147-02
Fixed Carbon Content	61.8	% ADB	ASTM D3175-02
Volatile Matter	36.5	% ADB	ASTM D3172-02
Calorie Number	7,044	cal/gr, ADB	ASTM D5865-03

Table 3 *Limestone composition*

Element	Ca	Mg	Si	Al	O
Wt%	43.01	0.57	6.51	2.43	33.93

Int. Journal of Integrated Engineering Vol. 16 No. 1 (2024) p. 26-34

2.2 Carbothermal Reduction Procedure

Prior to the carbothermic reduction process, all raw materials (nickel laterite, coal, and limestone) are crushed and ground until passing 50 standard mesh siever. Next, the nicke laterite fines, coal, and additives are mixed homogeneously using manual mixing. The mass portion in the mixing process is based on the mass balance calculation carried out previously. Since this research examined three different shapes, the briquette was formed into the pillow, spherical, and cylindrical shape (Fig. 2). The quantity of additive was 10% by weight so that selective reduction can take place as desired. After the mixing process, the binder (starch) and some waters are mixed together with nickel laterite, coal, and additives. Then, the mixed materials are fed into the mold cavity of the briquetting machine to make briquettes of different shapes. During briquetting, a pressure of 30 kgf/cm^2 was applied [14] to make 3 cm^3 volume of briquettes. After being released from the briquette mold, the green briquettes were dried at 100 ^{o}C for 3 h in an oven. Fig. 3 shows the XRD results of the limestone.

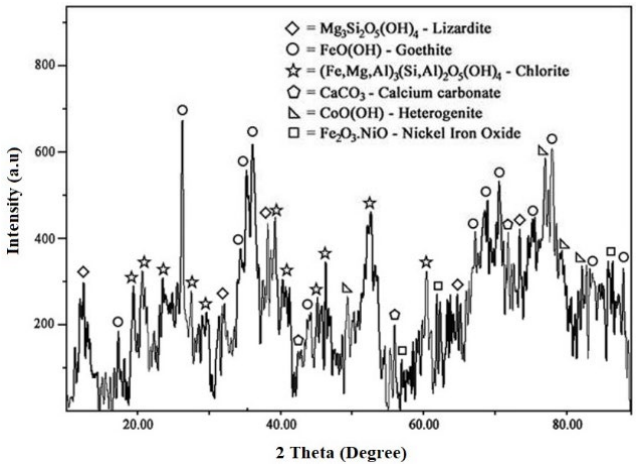

Fig. 1 *XRD diffractogram of laterite nickel*

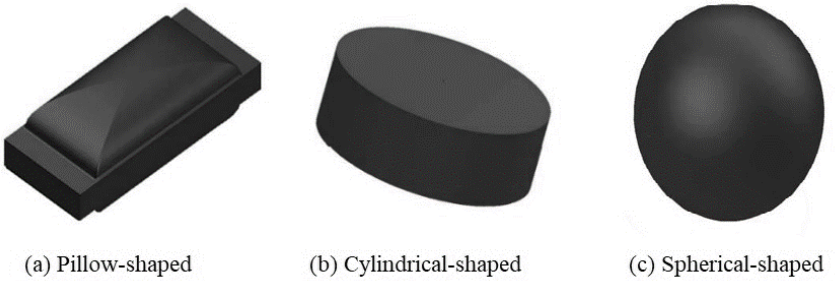

Fig. 2 *Briquette shape in this study*

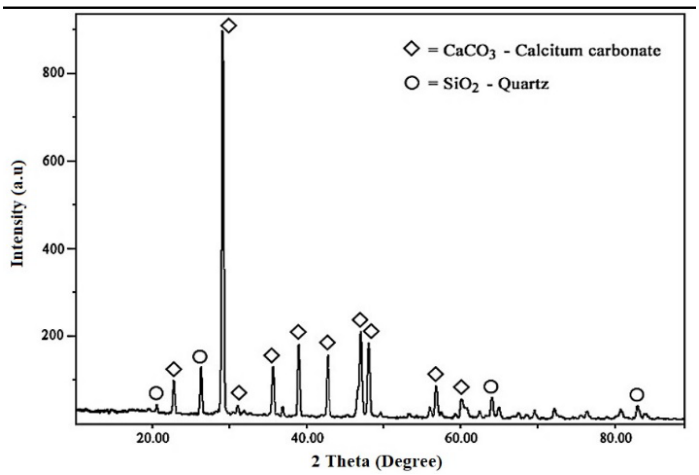

Fig. 3 *XRD pattern of limestone*

When preparing carbothermic reduction experiment, delicate coal-limestone blends were inlayed in the graphite crucible as the bed. After that, four briquettes (dried) of every sample were inserted into the crucible and subsequently covered by a layer of coal limestone. The carbothermal reduction was performed directly after the graphite crucible was inserted in a gas-type muffle furnace at 700 °C for 2 h to allow the dehydroxylation and continuous at 1400 °C for 6 h. After the reduction, the cooling process of the crucible was performed in the furnace until reaching ambient temperature. Before analysis, reduced briquettes were firstly crushed to approximately 1-2 mm size and followed by a magnetic separation (dry condition, 500 Gs) to classify a magnetic and non-magnetic portion.

2.3 Heat Transfer Analysis of Briquettes

The heat transfer was also considered in this study because the shape of the object will significantly affect heat transfer. Heat transfer analysis in this experiment can be done with Eq. 1.

$$Q = Q_{fuel} \times V \tag{1}$$

Where, Q is Heat transfer rate (J/s), Qfuel is Heat produced by fuel per volume (J/s.m3), and V is Briquette volume (m3). This equation was derived from Fourier's law. Eq. 2 describes the heat flux equation [22]. Then Eq. 2 is derived into Eq. 3. Eq. 3 can be derived further into Eq. 1. The heat transfer phenomenon here was assumed to occur in one dimensional steady state to simplify the phenomenon.

$$q = -k\frac{d\theta}{dx} \tag{2}$$

$$Q = -kA\frac{d\theta}{dx} \tag{3}$$

2.4 Reduced Product Characterizations

X-Ray Diffraction (XRD) characterization (PANalytical) with Cu Kα of 0.154 nm was conducted to evaluate the constituental phases of both magnetic and non-magnetic portion. In order to obtain the element constituent of each carbothermic reduced sample, a Scanning Electron Microscope-Emission Dispersive X-Ray (SEM-EDX) was performed. From this analysis, the elemental content in products and raw materials can be used to calculate the selectivity factor value according to Eq. 4. On the contrary, recovery of Ni and Fe were also estimated based on [23].

$$Selectivity\ Factor\ of\ Reduction = \frac{X_{Ni}Y_{Fe}}{X_{Fe}Y_{Ni}} \tag{4}$$

Where, X is the original elemental composition of iron and nickel in the nickel ore, and Y is the elemental composition of nickel and iron after carbothermal reduction process and separation by magnet. Table 4 shows the mass ratio of each raw material for this research.

Table 4 *This study used the mass ratio of raw materials for each briquette shape variation*

Variations	Mass ratio of Ore : Coal : Na_2SO_4 : Limestone : Binder
Pillow	100 : 60 : 21 : 58 : 4
Spherical	100 : 60 : 21 : 58 : 4
Cylindrical	100 : 60 : 21 : 58 : 4

3. Results and Discussion

3.1 Effect of Various Briquette Shapes on Heat Transfer Rate

The carbothermic reduction was carried out with various briquette shapes applied to determine the effect of the briquette shape on the heat transfer rate. The heat transfer rate of the briquette has been analyzed and calculated using Eq. 1. Fig. 4 shows the heat transfer rate of each briquette shape. From the result of heat transfer calculation, it is known that every briquette shape has different values due to differences in surface area and volume from variations in the shape of briquettes. This difference in the rate of heat transfer also affects the

Int. Journal of Integrated Engineering Vol. 16 No. 1 (2024) p. 26-34

rate of reduction, which affects the content and recovery of the product resulting from direct reduction. This heat transfer rate also signifies heat supplies received by the briquette so the reduction reaction can concur.

3.2 Effect of Various Briquette Shapes on Nickel and Iron Content of Reduced Products

After the carbothermic reduction process was conducted with shape of briquettes variation in the form of a pillow, cylindrical, and spherical, then to understand the influence of briquette shape variations on the elemental content of the magnetic portions, the EDX characterization was carried out. Table 5 and Fig. 5 show the results of the EDX characterization for Ni and Fe content from the reduced product.

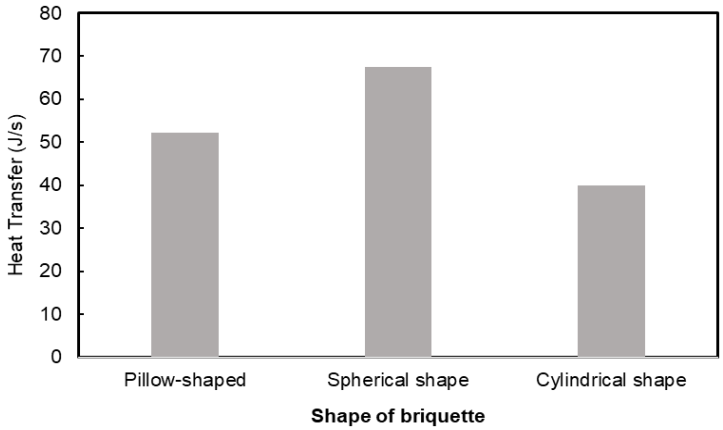

Fig. 4 *Heat transfer rate of each briquette shapes*

Table 5 *EDX Analysis of Reduced Limonitic Ore*

Variation	Ni Content (%)	Ni Mass (g)	Fe Content (%)	Fe Mass (g)
Pillow	5.00	1.38	27.06	7.47
Cylindrical	6.74	1.53	17.13	3.88
Spherical	4.02	1.05	22.96	6.00

The reduction of nickel and iron oxide in laterite nickel begins with the dehydroxylation process of Goethite and Lizardite (Eq. 5 and 6),

$$2(Fe,Ni)O.OH \rightarrow (Fe,Ni)_2O_3 + H_2O \quad (5)$$

$$Mg_3Si_2O_5(OH)_4 \rightarrow 3MgO + 2SiO_2 + 2\,H_2O \quad (6)$$

Then, the product of dehydroxilation reaction will continue with the reduction by CO gas (Eq. 7 and 8) [24].

$$NiFe_2O_4 + CO \rightarrow Ni + Fe_2O_3 + CO_2 \quad (7)$$

$$Fe_2O_3 + 3CO \rightarrow 2Fe + 3CO_2 \quad (8)$$

In addition, CO gas will react with Na_2SO_4, which act as a selective agent becomes Na_2S, S, and Na_2O (Eq. 9 and 10) [25].

$$Na_2SO_4 + 4CO \rightarrow Na_2S + 4CO_2 \quad (9)$$

$$Na_2SO_4 + 3CO \rightarrow Na_2O + S + 3CO_2 \quad (10)$$

This research is based on the effect that the shape of the briquettes will affect the rate of combustion due to differences in surface area. The difference in surface area will affect the reduction rate of the direct reduction process [26].

In pillow form, The Ni content obtained due to the heat transfer rate of the pillow model has an optimal heat transfer where the reduction rate of sulfur formation from additives is also optimal. In the spherical form, the cause of the low content of Ni obtained is because the combustion rate is slower than in the pillow and cylindrical forms, which causes less carbothermic reduction of products. In cylindrical form, the iron content produced is very small due to a large amount of iron reacting with sulfur which causes the iron content in the

reduced product to be smaller than the other variations. And this affects the nickel content, which is quite high compared to other variables. It is due to the high rate of heat transfer in the cylindrical form, which causes Na_2SO_4 to be easily reduced to Na_2O and sulfur, so a lot of Fe reacts with sulfur [27].

3.3 Effect of Various Briquette Shapes on Nickel and Iron Content of Reduced Products

The purpose of the carbothermic reduction process is to separate valuable minerals from worthless minerals. Recovery is a measuring tool to determine the quality of the carbothermal reduction process [19]. The recovery of nickel and iron is calculated by correlating the amount of each element in magnetic portion with its initial condition as raw material. The recovery determination in this research is established on the weight and composition of magnetic portion separated from a magnetic separation process. Fig. 6 shows the recovery of nickel and iron.

The optimal recovery value for nickel was obtained from the cylindrical shape, and the lowest recovery value was obtained from the spherical shape. It is because the spherical shape has the lowest heat transfer rate, and the cylindrical shape has the highest heat transfer rate compared to others. It also affects the reduction rate of Na_2SO_4 as an additive in the nickel laterite reduction process, where the function of the Na_2SO_4 additive is to bind Fe to increase the recovery of Ni from the selectivity process [25]. Fig. 6 also shows cylindrical shape has the lowest recovery value for iron. In addition to the effect of the additive, the reduction rate of limonitic laterite nickel ore is also affected by the rate of formation of CO gas as a reducing agent [21].

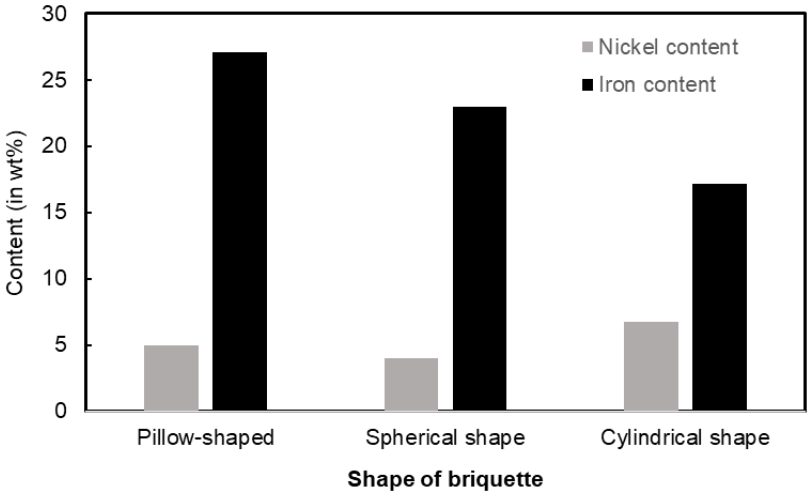

Fig. 5 *Nickel and iron content of each briquette shapes*

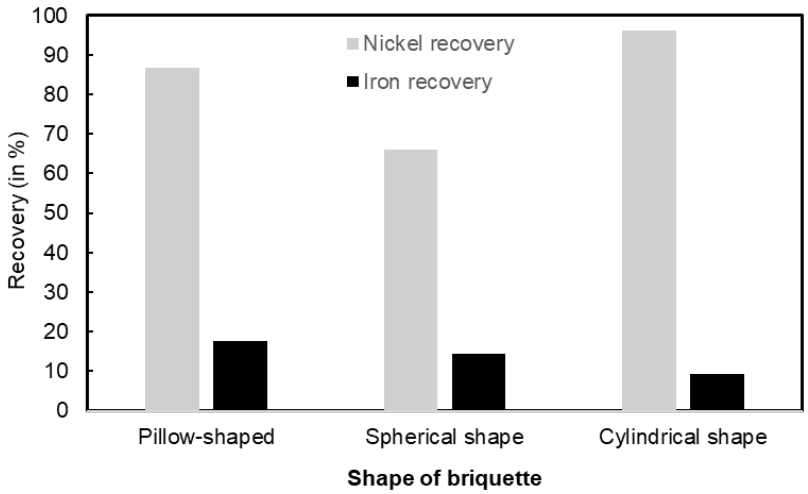

Fig. 6 *Recovery value of each briquette shapes*

Int. Journal of Integrated Engineering Vol. 16 No. 1 (2024) p. 26-34

3.4 Effect of Briquette Shapes on Compound Formed of Reduced Products

Fig. 7 shows the compound formed on reduced products. In each variation, the compound formed on the reduced product is Ferronickel (FeNi), Quartz (SiO_2), Forsterite (Mg_2SiO_4), and Fe_3Si. In the variation of the spherical shape, more forsterite (Mg_2SiO_4) compounds were found. It was due to the less-than-optimal reduction of Na_2SO_4. Mg_2SiO_4 is a product from recrystallization of lizardite that has undergone dehydroxylation. The recrystallization of Mg_2SiO_4 will occur when lizardite is subjected to higher temperature. It captures Ni and Fe in silica crystals resulting difficulty of these phases to be reduced in the next stage [28]. Because the reduction process is more difficult due to the low heat transfer rate, the Ni levels will also be lower. In spherical shape, forsterite and magnetite are also found due to a lack of sulfur supply from reduced Na_2SO_4. Therefore, it can be concluded that the reduction process in the spherical form is not perfect. The existence of Fe_3Si is because when the temperature reaches more than 1300°C, iron from limonite ore will form a reaction with reduced silica [29]. Fig. 7 indicates that nickel and iron can still be included even though Mg_2SiO_4 and Fe_3O_4 present [30].

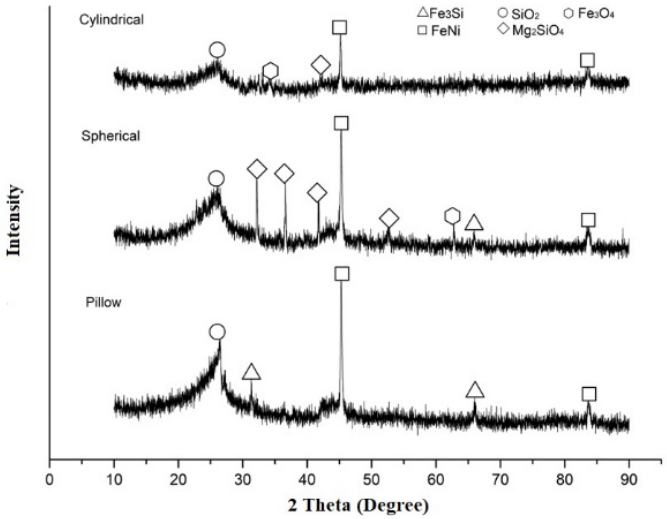

Fig. 7 *Compounds are formed on each briquette shape*

3.5 Selectivity Factor

By using Eq. 2, the selective reduction of nickel can be estimated by knowing the selectivity factor. Fig. 8 shows a selectivity factor graph from each variation of briquette shapes. In selective reduction, the selectivity factor is determined by the decomposition reaction of Na_2SO_4 as a reductive agent [31]. This decomposition occurs under reductive conditions, so it affects the decomposition process of Na_2SO_4, which produces Na_2O and sulphur. The selectivity factor will have an impact on the yield of the carbothermic reduction product. The selectivity factor can be used to show how effective the additive works when the reduction process occurs. In the variation of the briquette shape, the cylindrical shape has the best result, which is 10.39, followed by the pillow, which is 4.88, and spherical, which is 4.63. It is because the spherical variation has a low heat transfer rate compared to the pillow, which has an impact on the reduction rate of Na_2SO_4. However, further research needs to be conducted in the future to ascertain the effect of briquette shape on the selective reduction process.

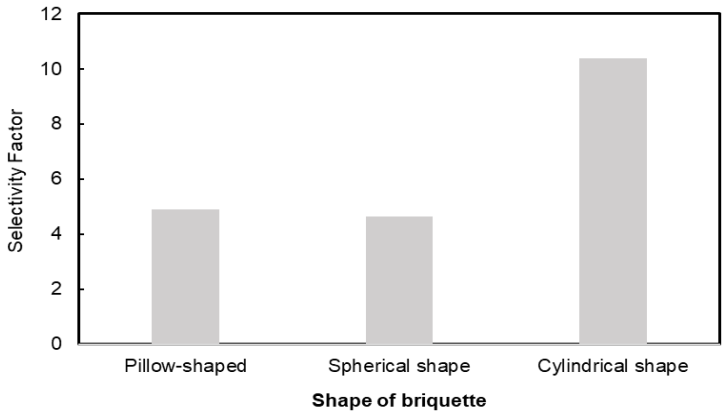

Fig. 8 *Selectivity factor value from each briquette shapes*

4. Conclusion

The shape of the briquettes affects the yield of the carbothermal reduction product due to the influence of the heat transfer rate experienced by each briquette. It is caused by different shapes having different volume and surface area values. The higher the volume of the briquette, the greater the heat transfer received by the briquettes. A high heat transfer rate causes limonitic laterite to be easily reduced into ferronickel as the final product. It also may cause the reduction of Na_2SO_4 as a selective reduction agent rapidly reacts with iron to form a non-magnetic compound which directly increases the content of nickel on the reduced product. The optimum reduced products achieved by cylindrical shape with nickel content and recovery were 6.74% and 96.20%, respectively. Selectivity factor affected by Na_2SO_4 additive role. It will react with Fe to form a non-magnetic product. These can be described by formed compounds that can show compounds formed on all variations. All variations show FeNi, which indicates the reduction of nickel and iron can occur. Forsterite (Mg_2SiO_4) and magnetite (Fe_3O_4) were found on the spherical shape, which causes the recovery value from the spherical shape to be lower than the other shape.

Acknowledgement

The authors express their highest appreciation to the Ministry of Education, Culture, Research, and Higher Education-Republic of Indonesia which has supported the funding of this research through the Penelitian Tesis Magister with a research main contract number: 084/E5/PG.02.00.PT/2022 and secondary contract number: 1464/PKS/ITS/2022 date: 10 May 2022.

Conflict of Interest

Authors declare that there is no conflict of interests regarding the publication of the paper.

Author Contribution

The authors confirm contribution to the paper as follows: **study conception and design:** FA, VAS, YS, SP; **data collection:** FA, AMYR, SP; **analysis and interpretation of results:** FA, AMYR, SP; **draft manuscript preparation:** FA, AMYR. All authors reviewed the results and approved the final version of the manuscript.

References

[1] Mudd, G. M., and Simon M. J. (2022) The New Century for Nickel Resources, Reserves, and Mining: Reassessing the Sustainability of the Devil's Metal. *Economic Geology 117 (8),* 1961–83. https://doi.org/10.5382/econgeo.4950.

[2] Tang, C., Benjamin S., Arnold T., and José M. M. (2021) The Impact of Climate Policy Implementation on Lithium, Cobalt and Nickel Demand: The Case of the Dutch Automotive Sector up to 2040. *Resources Policy 74*, 102351. https://doi.org/10.1016/j.resourpol.2021.102351.

[3] Guohua, Y., Ayman E., and Xi, X. (2021) Dynamic Analysis of Future Nickel Demand, Supply, and Associated Materials, Energy, Water, and Carbon Emissions in China. *Resources Policy 74*, 102432. https://doi.org/10.1016/j.resourpol.2021.102432.

[4] Farrokhpay, S., Lev F., and Daniel F. (2019) Pre-Concentration of Nickel in Laterite Ores Using Physical Separation Methods. *Minerals Engineering 141,* 105892. https://doi.org/10.1016/j.mineng.2019.105892.

[5] Yang, W., Baozhong M., Xiang L., Die H., Chengyan W., and Hua W. (2022) Transferring Behavior and Reaction Kinetics of Saprolitic Laterite during Metalized Reduction in the Presence of Calcium Fluoride. *Minerals Engineering 176*, 107353. https://doi.org/10.1016/j.mineng.2021.107353.

[6] Keskinkilic, E. (2019) Nickel Laterite Smelting Processes and Some Examples of Recent Possible Modifications to the Conventional Route. *Metals 9 (9),* 974. https://doi.org/10.3390/met9090974.

[7] Pandey, N., Sunil K.T., Sovan K.P., and Gaurav J. (2022) Recent Progress in Hydrometallurgical Processing of Nickel Lateritic Ore. *Transactions of the Indian Institute of Metals 76*, 11-30. https://doi.org/10.1007/s12666-022-02706-2.

[8] Tian, H., Zheng-qi G., Ruo-ning Z., Jian P., De-qing Z., Cong-cong Y., Liao-ting P., and Xue-zhong H. (2022) Upgrade of Nickel and Iron from Low-Grade Nickel Laterite by Improving Direct Reduction-Magnetic Separation Process. *Journal of Iron and Steel Research International 29 (8),* 1164–75. https://doi.org/10.1007/s42243-021-00646-7.

[9] Cao, Z., Baozhong M., Jiashun Z., Longfei S., Yongqiang C., and Chengyan W. (2022) Efficient Recovery of Iron and Chromium from Laterite Residue by Non-Molten Metallization Reduction. *Powder Technology 407*, 117618. https://doi.org/10.1016/j.powtec.2022.117618.

[10] Guo, X., Zhengyao L., Jicai H., Dong Y., and Tichang S. (2022) Petroleum Coke as Reductant in Co-Reduction of Low-Grade Laterite Ore and Red Mud to Prepare Ferronickel: Reductant and Reduction Effects.

International Journal of Minerals, Metallurgy and Materials 29 (3), 455–63. https://doi.org/10.1007/s12613-021-2389-9.

[11] Abdul, F., Devalini P.M., Setiyorini, Y., Setyowati, V.A., Pintowantoro, S. (2022) Effect of Inner Reductant Addition and Laying on Carbothermic Reduction Process of Laterite Nickel Ore/Coal Composite Briquette. *Arabian Journal for Science and Engineering 48*, 11285–11294. https://doi.org/10.1007/s13369-022-07402-3.

[12] Watanabe, T., Ono, S., Arai, H., Matsumori, T. (1987) Direct Reduction of Garnierite Ore for Production of Ferro-Nickel with a Rotary Kiln at Nippon Yakin Kogyo Co., Ltd., Oheyama Works. *International Journal of Mineral Processing 19 (1–4),* 173–87. https://doi.org/10.1016/0301-7516(87)90039-1.

[13] Abdul, F., Pintowantoro, S., Yuwandono, R.B. (2018) Analysis of Holding Time Variations to Ni and Fe Content and Morphology in Nickel Laterite Limonitic Reduction Process by Using Coal-Dolomite Bed. *AIP Conf. Proc.* 1945, 020033. https://doi.org/10.1063/1.5030255 .

[14] Abdul, F., Rare, F. G. L. L., Setiyorini, Y., Setyowati, V. A., Pintowantoro, S. (2023) Briquetting Pressure Roles in Selective Reduction Process of Limonitic Nickel Laterite. Key Engineering Materials 939, 3-9 https://doi.org/10.4028/p-rv871t

[15] Suharno, B., Nurjaman, F., Ramadini, C., Shofi, A. (2021) Additives in Selective Reduction of Lateritic Nickel Ores: Sodium Sulfate, Sodium Carbonate, and Sodium Chloride. *Mining, Metallurgy & Exploration 38 (5),* 2145–59. https://doi.org/10.1007/s42461-021-00456-1.

[16] Zhu, D., Pan, L., Guo, Z., Pan, J., Zhang, F. (2019) Utilization of Limonitic Nickel Laterite to Produce Ferronickel Concentrate by the Selective Reduction-Magnetic Separation Process. *Advanced Powder Technology 30 (2),* 451–60. https://doi.org/10.1016/j.apt.2018.11.024.

[17] Klaus M., Hermann, H.W., Bernd, F. (2018) Investigation of Processing of Pyrometallurgically Pre-Treated Lateritic Nickel Ores. In XXIX International Mineral Processing Congress. Moscow: Ore and Metals.

[18] Pintowantoro, S., Widyartha, A.B., Setiyorini, Y., Abdul, F. (2021) Sodium Thiosulfate and Natural Sulfur: Novel Potential Additives for Selective Reduction of Limonitic Laterite Ore. *Journal of Sustainable Metallurgy 7 (2),* 481–94. https://doi.org/10.1007/s40831-021-00352-4.

[19] Pintowantoro, S., Pasha R.A.M., Abdul, F., (2021) Gypsum Utilization on Selective Reduction of Limonitic Laterite Nickel. *Results in Engineering 12*, 100296. https://doi.org/10.1016/j.rineng.2021.100296.

[20] Abdul, F., Anhar, A.B., Setiyorini, Y., Setyowati, V.A., Pintowantoro, S. (2022) The Role of a Mixture of Coal and Dolomite in the Direct Reduction Process of Low-Grade Iron Sand Concentrate: A Pilot-Scale Study. *Transactions of the Indian Institute of Metals 75 (11),* 2969–2976. https://doi.org/10.1007/s12666-022-02685-4.

[21] Abdul, F., Pintowantoro, S., Hidayatullah, A.B. (2019) Analysis of Cylindrical Briquette Dimension on Total Iron Content and the Degree of Metallization in Direct Reduction Process of Iron Ore and Iron Sand Mixture. *Materials Science Forum 964,* 19–25. https://doi.org/10.4028/www.scientific.net/MSF.964.19.

[22] Iguchi, M., Olusegun J.I. (2014). Basic Transport Phenomena in Materials Engineering. Tokyo: Springer Japan. https://doi.org/10.1007/978-4-431-54020-5.

[23] Wills, BA, and JA Finch. 2016. Wills' Mineral Processing Technology. Elsevier. https://doi.org/10.1016/C2010-0-65478-2.

[24] Elliott, R., Pickles, C.A., Forster, J. (2016) Thermodynamics of the Reduction Roasting of Nickeliferous Laterite Ores. *Journal of Minerals and Materials Characterization and Engineering 04 (06),* 320–346. https://doi.org/10.4236/jmmce.2016.46028.

[25] Jiang, M., Sun, T., Liu, Z., Kou, J., Liu, N., Zhang, S. (2013) Mechanism of Sodium Sulfate in Promoting Selective Reduction of Nickel Laterite Ore during Reduction Roasting Process. *International Journal of Mineral Processing 123,* 32–38. https://doi.org/10.1016/j.minpro.2013.04.005.

[26] Narasingha, M.H., Suppamassadu, K.P. (2011) Effects of Bio-Coal Briquette Shape on Transport Phenomena in a Curing Unit by CFD Technique. Recent Advances in Fluid Mechanics and Heat and Mass Transfer - Proc. of the 9th IASME / WSEAS Int. Conf. on Fluid Mechanics and Aerodynamics, FMA'11, Proc. of the 9th IASME / WSEAS Int. Conf. HTE'11, 294–99.

[27] Liu, Z., Sun, T., Wang, X., Gao, E. (2015) Generation Process of FeS and Its Inhibition Mechanism on Iron Mineral Reduction in Selective Direct Reduction of Laterite Nickel Ore. *International Journal of Minerals, Metallurgy, and Materials 22 (9),* 901–906. https://doi.org/10.1007/s12613-015-1148-1.

[28] Setiawan, I,Febrina, E., Subagja, R., Harjanto, S., Firdiyono, F. (2019) Investigations on Mineralogical Characteristics of Indonesian Nickel Laterite Ores during the Roasting Process. *IOP Conference Series: Materials Science and Engineering 541 (1),* 012038. https://doi.org/10.1088/1757-899X/541/1/012038.

[29] Li, Q., Wei, Y., Li, B., Zhou, S., Wang, H., Ma, B., Wang, C. (2015) Phase Transformation in Magnesium-Rich Nickel Oxide Ore after Reduction Roasting Process. In 6th International Symposium on High-Temperature Metallurgical Processing, 297–304. Hoboken, NJ, USA: John Wiley & Sons, Inc. https://doi.org/10.1002/9781119093381.ch38.

[30] Kambuna, B. Hidayah, N., Triana, T., Supriyatna, Y.I., (2020) Analysis of Metal Phase Transformation and Particle Growth of the Reduction Ferronickel Plant Dust Pellet in Variations Temperature. *AIP Conf. Proc. 2232*, 060005. https://doi.org/10.1063/5.0001935.
[31] Widyartha, B., Setiyorini, Y., Abdul, F., Subakti, T. J., Pintowantoro, S. (2020) Effective beneficiation of low content nickel ferrous laterite using fluxing agent through Na_2SO_4 selective reduction. *Materialwissenschaft und Werkstofftechnik, 51(6),* 750-757. https://doi.org/10.1002/mawe.202000007